Effect of ligand structures on oxygen absorbability and viscosity of metal-containing ionic liquids

Matsuoka, Atsushi

Kamio, Eiji

Matsuyama, Hideto

(Citation)
Journal of Molecular Liquids,318:114365

(Issue Date)
2020-11-15

(Resource Type)
journal article

(Version)
Accepted Manuscript

(URL)
https://hdl.handle.net/20.500.14094/90007676

Effect of ligand structures on oxygen absorbability and viscosity of metal-containing ionic liquids

Atsushi Matsuoka, Eiji Kamio*, Hideto Matsuyama*

Research Center for Membrane and Film Technology, Department of Chemical Science and Engineering, Kobe University, 1-1 Rokkodai, Nada, Kobe 657-8501, Japan

*Corresponding author.
E-mail address: matuyama@kobe-u.ac.jp (H. Matsuyama)
E-mail address: e-kamio@people.kobe-u.ac.jp (E. Kamio)

Key words: Metal-containing ionic liquid, oxygen separation, viscosity, gas absorbability, π electron system

Abstract

Metal-containing ionic liquids (MCILs) composed of a cobalt(II) Schiff base complex and ionic-liquid-based axial ligands (ligand ILs) are potential O_2 absorbents. To determine the design criteria of MCILs with both highly selective O_2 absorbability and low viscosity, the relationship between the physicochemical properties and chemical structure of the MCILs was investigated. The measurement of the amount of O_2 absorbed in MCILs with various ligand ILs indicated that O_2 reactivity is determined by the electron density of the Co atom of the MCILs. The electron density of the Co atom could be controlled by the σ electron donation ability of the ligand ILs. Moreover, the viscosity of the MCILs was strongly affected by the interaction among the MCIL molecules caused by the π electron system. This interaction was weakened by the equatorially coordinating Schiff base and the ligand ILs within the chemical structure. Therefore, to develop MCILs with both high O_2 reactivity and low viscosity, suppression of the interaction caused by the π electron system without decreasing the electron density of the Co atom is important.

1. Introduction

O_2 separation from air is required in many industrial fields, such as medical[1], steel[2], and oxy-fuel combustions[2–4]. The current process for large-scale production of O_2 from air is a cryogenic method. Although almost 99% O_2 purity can be achieved by this process, it is complex and energy-intensive[2,3]. Conversely, O_2 absorption is a relatively small-scale and low energy consumption process, and has therefore attracted significant attention [2,5,6].

Recently, several metal-organic frameworks (MOFs) that can selectively absorb O_2 over N_2 were developed as O_2 absorbents [7,8]. Some MOFs with coordinately unsaturated metals showed high O_2 absorption and high O_2/N_2 absorption selectivity[9–13]. In contrast, ionic liquids (ILs) are promising as gas absorbent materials because of their negligible vapor pressure and the flexible design of their chemical structures[14–20]. Because the chemical structures of ILs can be easily modified, the physicochemical properties of ILs can be tuned for different applications [21–23]. For example, many task-specific ILs (TSILs), having functional groups that react with specific gas molecules, were developed as gas separation media[24,25,34,26–33]. Recently, we developed a novel metal-containing ionic liquid (MCIL; a type of TSIL) composed of an oxygen-absorbing metal complex, Co(salen) (salen= *N*, *N*'-bis(salicylidene)ethylenediamine) and an IL-based ligand (hereinafter denoted as ligand IL) that axially coordinates to Co(salen) (Fig. 1)[35]. The developed MCIL showed comparable or higher equilibrium absorption amounts of O_2 and O_2/N_2 absorption selectivity with respect to other O_2 absorbents[36]. Thus, this MCIL is one of the O_2 absorbent candidates for the establishment of a highly efficient O_2 absorption process.

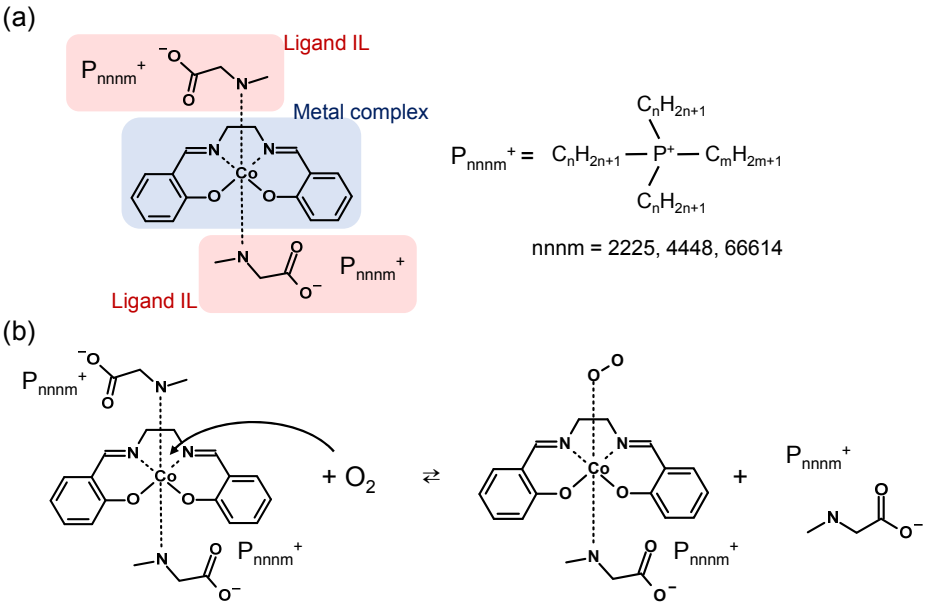

Fig. 1 (a) Chemical structure of O_2-absorbing MCILs developed in our previous work and (b) schematic illustration of predicted mechanism of reaction between O_2 molecules and MCILs

For the practical use of MCILs as O_2 absorbents, highly selective O_2 absorption and a high O_2 absorption rate are desired. A high O_2 absorption rate contributes to the downsizing of the O_2 absorption equipment. Although the selective O_2 absorbability of the MCILs developed by our group was satisfactory, the O_2 absorption rates were not so high. These low absorption rates were attributable to the high viscosity of the MCILs (20000-80000 mPa s). Therefore, for the practical application of the MCILs as O_2 absorbents, lower MCIL viscosity is desired.

The physicochemical properties of MCILs could be tuned by changing the chemical structures of the O_2-absorbing metal complex and the ligand ILs. The structure of the ligand ILs could be altered by changing the chemical structures of the cation and the anion. One coordinates to the metal and the other acts as a counter ion of the MCILs. Therefore, three parts of the MCILs, i.e. metal complex and the cation and anion of the ligand ILs, can be varied. It was reported that the physicochemical properties of MCILs could be controlled by the chemical structure of the MCIL counter ion [36,37]. However, the effects of the chemical structures of the metal complex and the ion which coordinates to the Co atom on MCIL properties have not yet been investigated.

In this study, new MCILs composed of two types of metal complexes and several ligand ILs were synthesized. The metal complexes used in this study were Co(salen) and Co(acacen) (acacen = *N*, *N*'-bis(acetylacetone)ethylenediamine). The ligand ILs are shown in Fig. 2. The properties of the synthesized MCILs that are most relevant to O_2 absorption, such as equilibrium absorption constants of O_2 and N_2 and viscosity, were investigated. From the results of O_2 and N_2 absorption equilibria, a dominant factor of the O_2 reactivity of the MCIL and that determines the amount of absorbed N_2 into the MCILs is revealed. In addition, based on the relationship between the chemical structure and viscosity of the MCILs, we considered that the interactions significantly affect the viscosity of the MCILs. Finally, guidelines for designing the optimal MCIL structure for O_2 absorption were proposed.

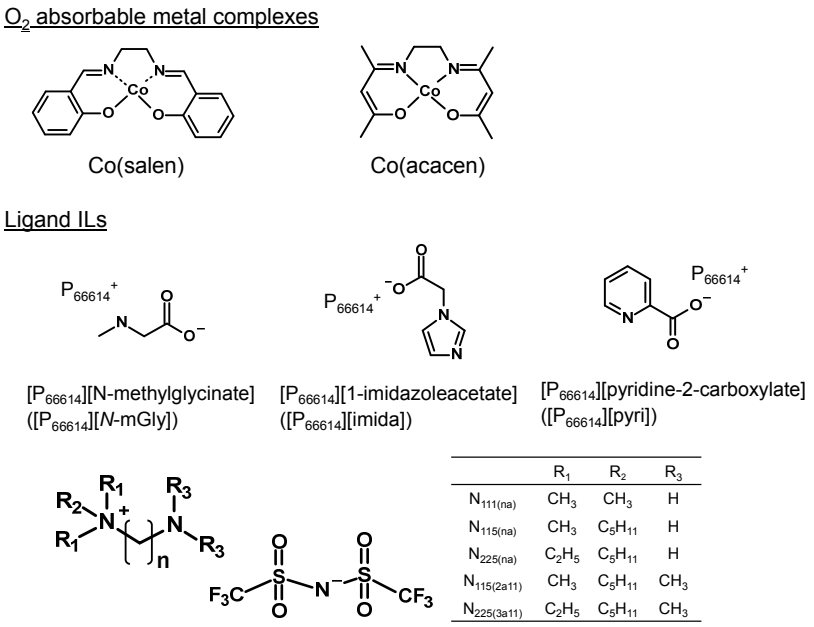

	R_1	R_2	R_3
$N_{111(na)}$	CH_3	CH_3	H
$N_{115(na)}$	CH_3	C_5H_{11}	H
$N_{225(na)}$	C_2H_5	C_5H_{11}	H
$N_{115(2a11)}$	CH_3	C_5H_{11}	CH_3
$N_{225(3a11)}$	C_2H_5	C_5H_{11}	CH_3

Fig. 2 Chemical structures of metal complexes and ligand ILs used in this study.

2. Experimental

2.1 Synthesis of MCILs

2.1.1 Reagents

Co(salen) (salcomine, >95%), as an O_2-absorbing metal complex, was purchased from Tokyo Chemical Industry Co. (Tokyo, Japan). Acetylacetone (>99.0%), ethylenediamine (99.0+%), and cobalt(II) acetate tetrahydrate ($Co(CH_3COO)_2 \cdot 4H_2O$; >99.0%), used for the synthesis of Co(acacen), were purchased from Tokyo Chemical Industry Co. (Tokyo, Japan), Wako Pure Chemicals Industry Ltd. (Osaka, Japan), and Nacalai Tesque, Inc. (Kyoto, Japan), respectively. *N*-methylglycine (>98%), 1-imidazoleacetic acid (>98%), and pyridine-2-carboxylic acid (>99.0%), used for the synthesis of $[P_{66614}][N\text{-mGly}]$, $[P_{66614}]$[imida], and $[P_{66614}]$[pyri], respectively, were purchased from Tokyo Chemical Industry Co. (Tokyo, Japan). Trihexyltetradecylphosphonium bromide ($[P_{66614}]$[Br], 95%) was purchased from Sigma-Aldrich Co. (St. Louis, MO, USA). Lithium bis(trifluoromethanesulfonyl)imide ($LiTf_2N$, >98%), used for the synthesis of $[N_{R1R1R2(naR3R3)}][Tf_2N]$, was purchased from Tokyo Chemical Industry Co. (Tokyo, Japan). 1,1,1-trimethylhydrazinium iodide ($[N_{111a}]$[I], 97%) was purchased from Sigma-Aldrich Co. (St. Louis, MO, USA). *N*,*N*-dimethylethylenediamine ($N_{11(2a)}$, >98.0%), *N*,*N*-dimethyl-1,3-propanediamine ($N_{11(3a)}$, >99.0%), *N*,*N*-diethylethylenediamine ($N_{22(2a)}$, >98.0%), *N*,*N*-diethyl-1,3-diaminopropane ($N_{22(3a)}$, >99.0%), and 1-bromopentane (>98.0%) used for the synthesis of $[N_{115(na)}]$[Br] and $[N_{225(na)}]$[Br] (n=2,3), and

2-bromoethylamine hydrobromide ($Br(CH_2)_2NH_2 \cdot HBr$, >98.0%), 3-bromopropylamine hydrobromide ($Br(CH_2)_3NH_2 \cdot HBr$, >98.0%), and trimethylamine (2 mol dm^{-3} in tetrahydrofuran) used for the synthesis of $[N_{111(na)}][Br]$ (n=2,3), were purchased from Tokyo Chemical Industry Co. (Tokyo, Japan). 1,1-dimethylhydrazine (>98.0%), used for the synthesis of $[N_{115a}][Br]$, was purchased from Tokyo Chemical Industry Co. (Tokyo, Japan). Di-tert-butyl decarbonate ($(Boc)_2O$; >95%) for boc protection of amine was purchased from Tokyo Chemical Industry Co. (Tokyo, Japan). Paraformaldehyde (>90%) and formic acid (98%) for the Eschweiler-Clarke reaction were purchased from Tokyo Chemical Industry Co. (Tokyo, Japan) and Wako Pure Chemicals Industry Ltd. (Osaka, Japan), respectively. Ethanol (99.5%), methanol (99.5%), acetonitrile (99.5%), tetrahydrofuran (stabilizer free, 99.5%), hexane (96%), dichloromethane (99.5%), diethylether (99.5%) sodium hydroxide (5 mol dm^{-3} in aqueous solution), and 0.5 mol dm^{-3} hydrochloric acid methanolic solution were purchased from Wako Pure Chemicals Industry Ltd. (Osaka, Japan). The anion-exchange resin (Amberlite IRN78, hydroxide form) used for the anion-exchange reaction of $[P_{66614}][Br]$ was purchased from Sigma-Aldrich Co. (St. Louis, MO, USA). All reagents were used as received.

2.1.2 Synthesis of MCILs

The ligand ILs were synthesized as follows. $[P_{66614}][N\text{-mGly}]$, $[P_{66614}][imida]$, and $[P_{66614}][pyri]$ were synthesized by neutralization according to a method reported elsewhere [38]. First, $[P_{66614}][OH]$ was synthesized by anion exchange of $[P_{66614}][Br]$ using an anion-exchange resin. Then $[P_{66614}][N\text{-mGly}]$, $[P_{66614}][imida]$, and $[P_{66614}][pyri]$ were synthesized by a neutralization reaction between $[P_{66614}][OH]$ and *N*-methylglycine, $[P_{66614}][OH]$ and 1-imidazoleacetic acid, and $[P_{66614}][OH]$ and pyridine-2-carboxylic acid, respectively.

$[N_{R1R1R2(na)}][Tf_2N]$ were synthesized by the anion-exchange reaction between $[N_{111a}][I]$ or $[N_{R1R1R2(naR3R3)}][Br]$ and $LiTf_2N$. Except for commercially available $[N_{111a}][I]$, $[N_{R1R1R2(naR3R3)}][Br]$ were synthesized. Before the synthesis of $[N_{115(na)}][Br]$, $[N_{225(na)}][Br]$, and $[N_{111(na)}][Br]$ (n = 2,3), the amino group of $N_{11(na)}$, $N_{22(na)}$, and $Br(CH_2)_nNH_2$ (n=2,3) was protected by a boc group. $[N_{115(na)}][Br]$ and $[N_{225(na)}][Br]$ (n = 2,3) were synthesized by reacting boc-protected $N_{11(na)}$ or boc-protected $N_{22(na)}$ with 1-bromopentane, followed by deprotection of the boc group. $[N_{111(na)}][Br]$ (n=2,3) were synthesized by a reaction between boc-protected $Br(CH_2)_nNH_2$ (n=2,3) and trimethylamine, followed by boc deprotection. $[N_{115a}][Br]$ was synthesized by the reaction between dimethylhydrazine and 1-bromopentane. $[N_{225(3a11)}][Br]$ and $[N_{115(2a11)}][Br]$ were synthesized by dimethylation of $[N_{225(3a)}][Br]$ and $[N_{115(2a)}][Br]$, respectively. For dimethylation, the Eschweiler-Clarke reaction with formaldehyde and formic acid[39] was used. The details of the synthesis of all ligand ILs are described in the Supporting information.

Acacen, used as the equatorial ligand of the Co(acacen)-type MCILs, was synthesized according to a previously reported method[40]. A solution of ethylenediamine (50 mmol) dissolved in 10 cm^3 of

ethanol was added dropwise to a solution of acetylacetone (100 mmol) in 30 cm^3 of ethanol. The mixture was stirred for 5 h at 298 K. After 5 h, a white precipitate was obtained and collected by filtration. The precipitate was then recrystallized using 20 cm^3 of ethanol. The Co(salen)-type MCILs were synthesized according to our previous report[35]. A solution of ligand ILs (4.0 mmol) dissolved in 5.0 cm^3 of ethanol was added dropwise into a suspension of Co(salen) (2.0 mmol) in 5.0 cm^3 of ethanol. The mixture was stirred for 5 h at 303 K under a N_2 atmosphere. After 5 h, the unreacted Co(salen) was removed by filtration. Then, ethanol was removed by N_2 bubbling for 12 h. The absence of ethanol in the obtained MCILs was confirmed by Fourier transform infrared (FT-IR) spectroscopy (Supporting information).

The Co(acacen)-type MCILs were synthesized by the modification of a previously reported procedure[41]. A solution of ligand ILs (4.0 mmol) dissolved in 5.0 cm^3 of ethanol was added to a solution of $Co(CH_3COO)_2 \cdot 4H_2O$ (2.0 mmol) and acacen (2.0 mmol) dissolved in 5 cm^3 of ethanol. The mixture was stirred for 5 h at 303 K under a N_2 atmosphere. After 5 h, the ethanol and acetic acid were removed by N_2 bubbling for 12 h. The absence of ethanol and acetic acid in the obtained MCILs was confirmed by FT-IR measurement (Supporting information).

2.2 Measurement of density and viscosity of the MCILs

The densities of the MCILs were determined by measuring the weight of a known volume of MCIL. A gas-tight syringe (No. 1725, Hamilton Co., Reno, NV) with a volume of 0.25 cm^3 was used for the density measurement. A constant volume of the MCIL (0.15 cm^3) was collected in the gas-tight syringe and weighed at 303.0 K.

The viscosity of the MCILs after O_2 absorption was measured using a rheometer (MCR 501, Anton Paar Co. Ltd.) with a cone plate (CP25-2, Anton Paar Co. Ltd.) at 303.0 K. Because the viscosity of the MCILs showed the constant value for the shear rate below 100 s^{-1}, the shear rate for the measurement was set to 10 s^{-1}.

2.3 Measurement of equilibrium absorption amounts of O_2 and N_2 in the MCILs

The amounts of O_2 and N_2 absorbed in the MCILs were measured by our previously reported method[24]. The gas absorption apparatus was composed of stainless-steel tubes and reference and sample cells. The temperature of the system was kept constant using a water bath (T-105B; Thomas Kagaku Co., Ltd., Tokyo, Japan). The MCILs used for the gas absorption test were degassed in advance to remove absorbed O_2 from the air. The MCIL/ethanol solution was prepared by adding 5 cm^3 of ethanol, with O_2 removed by N_2 bubbling, to 1 g of the degassed MCILs under a N_2 atmosphere.

The reference and sample cells were degassed under vacuum for more than 1 h to remove air, followed by charging with pure N_2 (about 100 kPa) to completely remove the considerable amount of O_2 that remained in the apparatus. Subsequently, the sample cell filled with N_2 was sealed by closing

the 2-way valve, detached, and weighed. The prepared MCIL/ethanol solution was loaded into the sample cell through the septum using a syringe. Then the sample cell was reattached to the system. The system was maintained at 333.0 K and vacuumed for 48 h to remove ethanol. The elimination of ethanol from the MCIL was confirmed by the pressure change in the system, i.e. the ethanol was deemed to be completely removed when the pressure no longer changed. Subsequently, N_2 was charged into the system again (about 100 kPa), and the sample cell filled with N_2 was detached and weighed in the same manner as described above. The weight of the MCIL loaded in the sample cell was calculated by the weight difference of the sample cell before and after MCIL loading.

After attaching the MCIL-loaded sample cell to the system, the temperature was maintained at 303.0 K. Then, the system was fully evacuated to completely remove the charged N_2. After the degasification of the system, the valve connecting the two cells was closed. The reference cell was then pressurized to charge a known amount of O_2 or N_2. After the gas was charged, the MCIL was constantly stirred using a stirrer throughout the experiment. Gas absorption was initiated by opening the valve connecting the two cells to introduce the gas charged in the reference cell into the sample cell. The pressure drop along with the gas absorption by the MCIL was measured using a digital pressure gauge (Model AM-756 digital manometer, GE Sensing & Inspection Technologies Co., Ltd.). The pressure was monitored until it became constant. It took about 150 h and 24 h to reach equilibrium for O_2 and N_2, respectively. After equilibration was attained, the amount of gas absorbed in the MCIL was determined from the initial and equilibrated pressures.

2.4 Determination of pK_a of the ligand ILs

A 300 cm^3 glass vial was used as a titration vessel. A solution of the ligand IL (200 cm^3, 10 mmol) in methanol (MeOH) was poured into the glass vial, and the temperature was maintained at 303.0 K using a water bath (TBX182SA, ADVANTEC). The pH of the solution was measured by a pH meter (pH meter: LAQUA F-74 electrode: 6377-10D, HORIBA, Ltd.) calibrated by aqueous standard solutions (pH standard solutions (pH 7, pH 9), HORIBA Advanced Techno Co., Ltd.). Because the pH meter was calibrated by an aqueous buffer, the pH value of the methanol solution measured by the pH meter (pH_{obs}) should be corrected. Based on the previous report[42], the actual pH value of the methanol solution (pH_{MeOH}) can be determined by the following equation;

$$pH_{MeOH} = pH_{obs} + 2.24$$

The ligand IL/MeOH solution was titrated with 0.5 mol dm^{-3} hydrochloric acid methanolic solution in 1 cm^3 or 0.5 cm^3 steps. Neutralization titration curves of each ligand IL were obtained by plotting the pH_{MeOH} values against the titrated volume of the hydrochloric acid methanolic solution. The pK_a

values of the ligand ILs were determined by analyzing the titration curves by the method described in the Supporting information.

3. Results and Discussion

3.1 Equilibrium gas absorption

3.1.1 N_2 absorption

To achieve high O_2/N_2 absorption selectivity, the amount of absorbed N_2 in the MCILs should be decreased. Therefore, we firstly investigated how the chemical structure of the MCILs affects N_2 absorption by the MCILs. To investigate the relationship between the chemical structure of the MCILs and the amount of absorbed N_2, the N_2 absorption of several MCILs were measured. Fig. 3 shows the N_2 absorption isotherms of each MCIL at 303.0 K. The amount of absorbed N_2 in the MCILs increased linearly with increasing N_2 pressure, i.e. N_2 was physically absorbed in the MCILs according to Henry's law. The Henry's constants of the MCILs (H_{N2} (mol dm^{-3} kPa^{-1})), determined from the slopes shown in Fig. 3, are listed in Table 1.

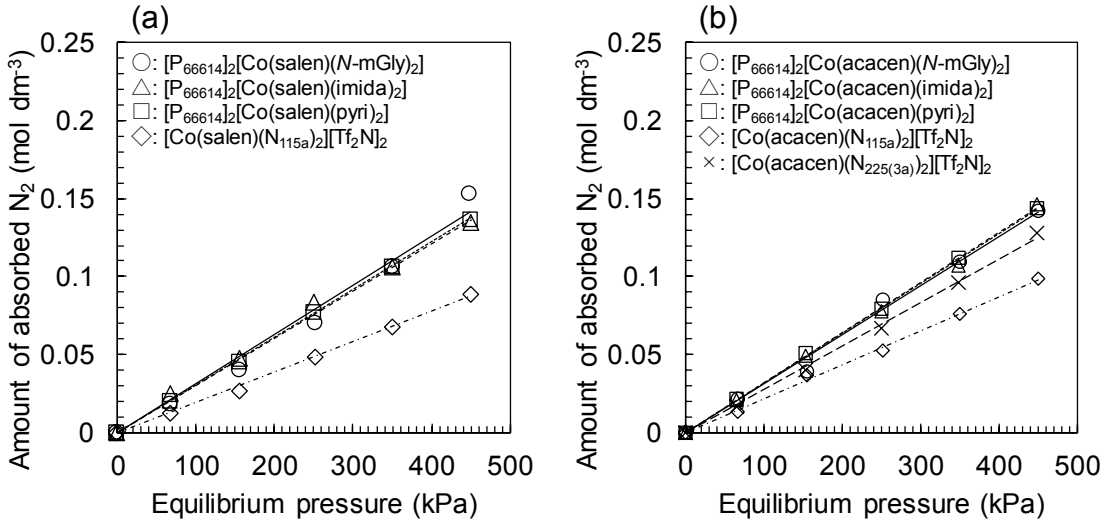

Fig. 3 N_2 absorption isotherms of (a) Co(salen)-type and (b) Co(acacen)-type MCILs with several ligand ILs at 303.0 K. The data of $[P_{66614}]_2$[Co(salen)(*N*-mGly)$_2$] are previously reported in ref. 32

Table 1 Molecular weight, density, molar volume, and H_{N2} of each MCIL at 303.0 K.

MCILs	Molecular weight (g mol^{-1})	Density (g·cm^{-3})	Molar volume (cm^3·mol^{-1})	$H_{N2}\times10^4$ (mol dm^{-3} kPa^{-1})
$[P_{66614}]_2[Co(salen)(N\text{-mGly})_2]$	1469.11	1.02	1440	3.14
$[P_{66614}]_2[Co(salen)(imida)_2]$	1545.17	1.07	1444	3.07
$[P_{66614}]_2[Co(salen)(pyri)_2]$	1539.16	1.06	1452	3.02
$[Co(salen)(N_{115a})_2][Tf_2N]_2$	1150.01	1.42	809	1.94
$[P_{66614}]_2[Co(acacen)(N\text{-mGly})_2]$	1425.10	1.01	1410	3.15
$[P_{66614}]_2[Co(acacen)(imida)_2]$	1501.16	1.02	1471	3.18
$[P_{66614}]_2[Co(acacen)(pyri)_2]$	1495.15	0.97	1541	3.21
$[Co(acacen)(N_{115a})_2][Tf_2N]_2$	1106.00	1.18	937	2.18
$[Co(acacen)(N_{225(3a)})_2][Tf_2N]_2$	1244.25	1.12	1110	2.79

For general room-temperature ILs (RTILs), the effect of the chemical structure of the RTILs on the amount of physically absorbed gas was investigated [43]. It was revealed that in the case of physical absorption where no chemical reaction was occurred between the RTIL and the gas molecules, a large free volume, which is related with the molar volume of RTILs, resulted in a large amount of gas absorption[44,45]. Fig. 4 shows the relationship between H_{N2} and the molar volumes of MCILs calculated from the molecular weight and density of the MCILs (Table 1). The H_{N2} of MCILs increased with increasing MCIL molar volume. Furthermore, both Co(acacen)-type and Co(salen)-type MCILs followed the same trend. This result indicated that the molar volume of MCILs is a critical factor determining the amount of N_2 absorbed in the MCILs. In other words, other factors, such as the compatibility of MCILs with N_2, had a small effect on the H_{N2}. Therefore, to obtain low N_2 absorption amount, the molar volume of the MCILs should be low[46]. Thus, the design of MCILs with low N_2 absorption amount requires the use of small O_2-absorbing metal complexes and small ligand ILs.

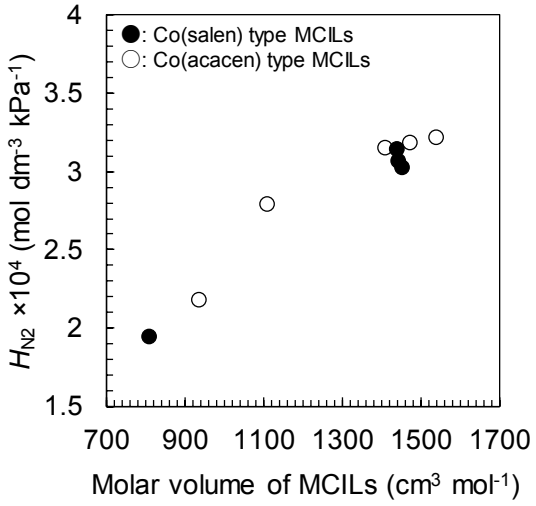

Fig. 4 Relationship between Henry's constants of N_2 absorption at 303.0 K and molar volume of MCILs.

3.1.2 O_2 absorption

In our previous research, it was clarified that the equilibrium relationship between the MCILs and O_2 can be described by the following equations[36];

$$O_2(gas) \rightleftharpoons O_2(MCIL), \qquad H_{O2} \quad \text{(physical absorption)} \tag{1}$$

$$Co(EL)\cdot L_2 + O_2(MCIL) \rightleftharpoons Co(EL)\cdot L\cdot O_2 + L, \qquad K_1 \tag{2}$$

$$Co(EL)\cdot L\cdot O_2 + Co(EL)\cdot L_2 \rightleftharpoons (Co(EL)\cdot L)_2\cdot O_2 + L, \qquad K_2 \tag{3}$$

where $Co(EL)\cdot L_2$ is the MCIL. Co(EL) is the O_2-absorbing complex (Co(acacen) and Co(salen)), and L is the ligand IL. H_{O2} (mol dm^{-3} kPa^{-1}) is Henry's constant of the physical O_2 absorption in the MCIL. K_1 (-) and K_2 (-) are the absorption equilibrium constants for Eqs. 2 and 3, respectively. It is clear from Eqs. 2 and 3, that large K_1 and K_2 lead to a large amount of absorbed O_2. The K_1 and K_2 of each MCIL were determined by analyzing the O_2 absorption isotherms of each MCIL obtained from the O_2 absorption tests.

The O_2 absorption isotherms of the MCILs measured at 303.0 K are shown in Fig. 5. The lines in Fig. 5 are the theoretical absorption isotherms calculated based on Eqs. 1-3. The determined parameters, H_{O2}, K_1, and K_2, are listed in Table 2. The K_2 values of all MCILs were very small. This indicated that the synthesized MCILs hardly formed $(Co(EL)\cdot L)_2\cdot O_2$. In other words, the formation of the $Co(EL)\cdot L\cdot O_2$ complex was dominant. Therefore, K_1 could be used to evaluate the O_2 reactivity of the MCILs.

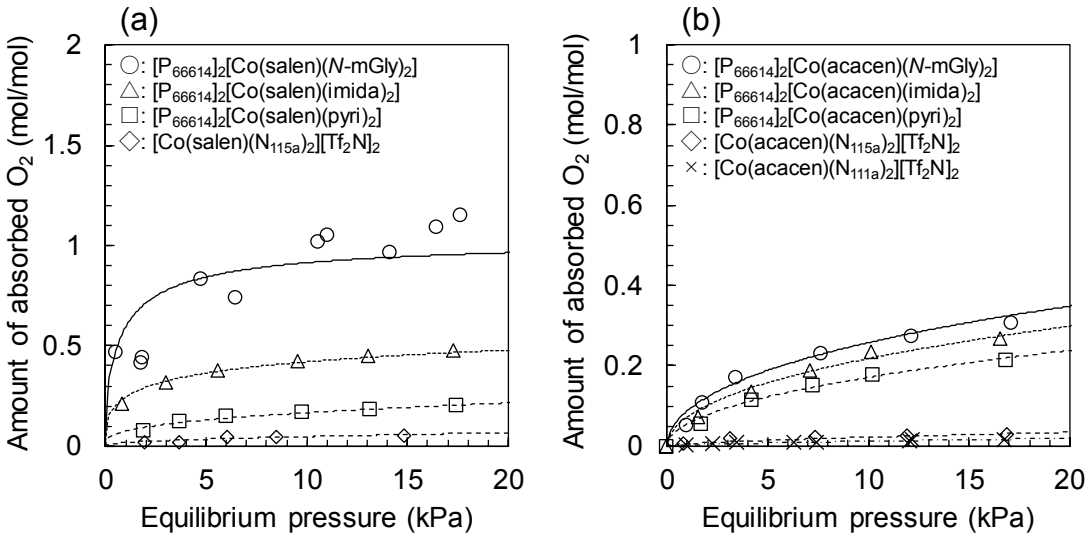

Fig. 5 O_2 absorption isotherms of (a) Co(salen)-type and (b) Co(acacen)-type MCILs with several ligand ILs at 303.0 K. The data of the $[P_{66614}]_2[Co(salen)(N\text{-mGly})_2]$ are those previously reported in ref. 32

Table 2 Equilibrium constants of O_2 absorption in MCILs at 303.0 K.

MCILs	$H_{O2}\times10^4$ (mol dm^{-3} kPa^{-1})	K_1 (-)	K_2 (-)
$[P_{66614}]_2[Co(salen)(N\text{-mGly})_2]$	5	1200	< 0.001
$[P_{66614}]_2[Co(salen)(imida)_2]$	5	50	< 0.001
$[P_{66614}]_2[Co(salen)(pyri)_2]$	5	6.5	< 0.001
$[Co(salen)(N_{115a})_2][Tf_2N]_2$	3.33	0.4	< 0.001
$[P_{66614}]_2[Co(acacen)(N\text{-mGly})_2]$	5	12	< 0.001
$[P_{66614}]_2[Co(acacen)(imida)_2]$	5	7.5	< 0.001
$[P_{66614}]_2[Co(acacen)(pyri)_2]$	5	4.3	< 0.001
$[Co(acacen)(N_{111a})_2][Tf_2N]_2$	3.33	0.025	< 0.001
$[Co(acacen)(N_{115a})_2][Tf_2N]_2$	3.33	0.1	< 0.001

As shown in Fig. 5 and Table 2, for both Co(acacen) and Co(salen)-type MCILs, the amount of absorbed O_2 and K_1 increased with a change of ligand ILs in the order of $[P_{66614}][N\text{-mGly}] > [P_{66614}][imida] > [P_{66614}][pyri] > [N_{115a}][Tf_2N]$. Carter et al. investigated the effect of the axial ligand on the O_2 reactivity of solutions of the Co(acacen) complex with various axial ligands[47]. In their report, they revealed that an axial ligand coordinating to Co(acacen) could enhance the electron density of the Co atom, and the O_2 reactivity of Co(acacen) was increased mainly by σ electron donation from the axial ligand. This means that the high electron donation ability of the axial ligand imparts high O_2

absorbability to the Co(acacen) complex. The σ electron donation from the axial ligand also enhances the reactivity of the Co(salen) complex[48].

In MCILs, the ligand ILs axially coordinate to the Co atom. Therefore, the σ electron donation ability of the ligand ILs could strongly affect the O_2 absorbability of both Co(acacen) and Co(salen)-type MCILs. Because the pK_a of the conjugate acid could be taken as a measure of the σ electron donation ability of axial ligands[47,49], the pK_a value of the ligand ILs could be used as an indicator of their σ electron donation ability.

Fig. 6 shows the relationship between log K_1 of the MCILs and the pK_a of the ligand ILs. As shown in Fig. 6, the values of log K_1 of both Co(acacen)-type and Co(salen)-type MCILs increased with an increase of ligand IL pK_a. Therefore, it can be said that the pK_a value related to the σ electron donation ability of the ligand ILs strongly affects the O_2 reactivity of both types of MCILs. Thus, to synthesize MCILs with high O_2 absorbability, highly electron donating ligand ILs should be used.

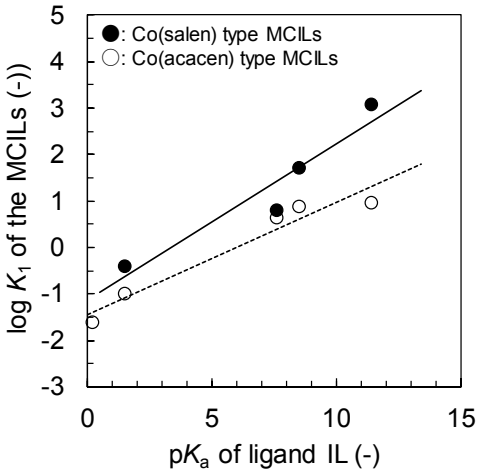

Fig. 6 Relationship between log K_1 of MCILs and pK_a of ligand ILs measured by acid-base titration test in methanol solution at 303.0 K.

In contrast, as shown in Fig. 6, comparison of the log K_1 of MCILs with the same ligand ILs shows that the Co(salen)-type MCILs have larger K_1 values than those of the Co(acacen)-type MCILs. This indicates that the O_2 reactivity of Co(acacen)-type MCILs was lower than that of Co(salen)-type MCILs. It was reported that the O_2 reactivity of the Co(acacen) complex solution was higher than that of the Co(salen) solution[50]. The result obtained showed the opposite trend. Crumblis et al. reported that the O_2 absorbability of Co(acacen) was deactivated because of some catalytic reaction between Co(acacen) and the organic ligand at room temperature[49]. Therefore, one possible reason to explain the lower O_2 reactivity of Co(acacen)-type MCILs than that of Co(salen)-type MCILs might be the deactivation of Co(acacen)-type MCILs at 303.0 K.

3.2 Viscosity of MCILs

Since the interaction among MCIL molecules strongly affect the viscosity of MCILs, investigation on this interaction was expected to shed light on the optimal chemical structure for MCILs with low viscosity. To evaluate the intermolecular interaction, some report adopted the friccohesity that is a ratio of the cohesive force and frictional force[51–53]. Friccohesity is calculated by $\sigma = \eta/\gamma$, where η and γ are the viscosity and surface tension of the solution, respectively. However, the viscosity of the MCILs used in this study were very high, the surface tension of the MCILs could not be measured. Therefore, only the viscosity of the MCILs was adopted for the indicator of the interaction between the MCIL molecules.

Fig. 7 shows the viscosities of the Co(acacen)-type and Co(salen)-type MCILs with different ligand ILs ([P_{66614}][*N*-mGly], [P_{66614}][imida], [P_{66614}][pyri], and [N_{115a}][Tf_2N]). Comparing the viscosity of MCILs with the same ligand ILs, the viscosity of Co(acacen)-type MCILs was lower than that of Co(salen)-type MCILs. This difference could be attributed to the difference in chemical structure of the equatorial ligands. The important difference in the chemical structures of acacen and salen is the existence of an aromatic ring (Fig. 2): salen has an aromatic ring, while acacen does not. The π electron system including an aromatic ring could cause intermolecular interactions such as cation-π interaction, NH-π interaction, CH-π interaction, and π-π interaction (hereinafter, these interactions are expressed as X-π interactions). It was reported that X-π interactions are important non-covalent intermolecular forces and play a significant role in the building or conformation of molecules[54,55]. It was also reported that X-π interactions govern the crystal structure of some metal complexes, including Co(salen) and its derivatives[56–59]. Therefore, X-π interactions among the MCIL molecules caused by the π electron system of equatorial ligands might affect the viscosity of MCILs.

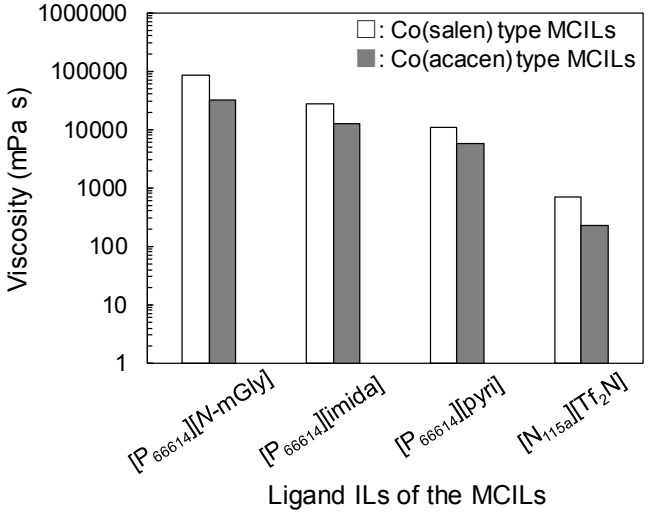

Fig. 7 Viscosities of both types of MCILs with several ligand ILs at 303.0 K

It was known that the strength of intermolecular X-π interactions increases with an increase in the extent of the π electron system[60]. Although the acacen ligand also has a π electron system, the salen ligand, which has a wide π electron system because of the aromatic ring, causes stronger intermolecular interactions among MCIL molecules than the acacen ligand. The higher density of Co(salen)-type MCILs than that of Co(acacen)-type MCILs (Table 1) suggested that Co(salen)-type MCIL molecules strongly interact with each other. Therefore, the higher viscosity of Co(salen)-type MCILs could be caused by the stronger X-π interactions among Co(salen)-type MCIL molecules.

In contrast, the viscosities of both types of MCILs were changed by the types of ligand ILs coordinating to the metal complexes. MCIL viscosity increased in the order of $[P_{66614}][N\text{-mGly}] > [P_{66614}][\text{imida}] > [P_{66614}][\text{pyri}] > [N_{115a}][Tf_2N]$. As mentioned above, X-π interactions determine the viscosity of MCILs. Therefore, the change in MCIL viscosity with different ligand ILs means that the ligand ILs might affect the strength of X-π interactions among MCIL molecules. The ligand ILs could affect the strength of X-π interactions by the following mechanism. The equatorial ligand withdraws the electrons of the Co atom[47,56]. Therefore, the higher electron density of the Co atom increases the electron density of the π electron system of the equatorial ligands. In general, the strength of the X-π interactions increases with increasing π electron density[61,62]. The axially coordinating ligand ILs could increase the electron density of the MCIL Co atom by σ electron donation. Therefore, the π electron density of the MCIL equatorial ligand increases with an increase in the σ electron donation ability of the ligand ILs (Fig. S7).

According to this consideration, higher π electron density of equatorial ligands due to the high σ electron donation ability of ligand ILs might cause higher MCIL viscosity. In fact, as shown in Table 3, the viscosity of MCILs increases with an increase of pK_a of the ligand ILs. Here, pK_a is the indicator of the σ electron donation ability of the ligand ILs[47,49]. Therefore, the above-mentioned speculation can explain the trend of MCIL viscosity with different ligand ILs.

Table 3 pK_a values of ligand ILs and corresponding MCIL viscosity.

MCILs	pK_a of ligand IL (-)	Viscosity of MCIL (mPa s)
$[P_{66614}]_2[Co(salen)(N\text{-mGly})_2]$	11.4	83150
$[P_{66614}]_2[Co(salen)(imida)_2]$	8.5	28280
$[P_{66614}]_2[Co(salen)(pyri)_2]$	7.6	10720
$[Co(salen)(N_{115a})_2][Tf_2N]_2$	1.5	706
$[P_{66614}]_2[Co(acacen)(N\text{-mGly})_2]$	11.4	31448
$[P_{66614}]_2[Co(acacen)(imida)_2]$	8.5	12500
$[P_{66614}]_2[Co(acacen)(pyri)_2]$	7.6	5740
$[Co(acacen)(N_{115a})_2][Tf_2N]_2$	1.5	229

To obtain evidence to support this speculation, IR spectra of MCILs with different ligand ILs were measured. Fig. 8(a) shows the IR spectra of neat Co(salen) and Co(salen)-type MCILs with different ligand ILs. The peaks observed around 1450 cm^{-1} for neat Co(salen) and each Co(salen)-type MCIL were assigned to the aromatic C=C bond of Co(salen) (ν(C=C))[63]. As shown in Fig. 8(a), ν(C=C) of the MCILs were shifted to higher wavenumbers than that of the neat Co(salen) complex. The wavenumber shift for each MCIL from the neat Co(salen) complex, $\Delta\nu$(C=C) was plotted against the pK_a value of the ligand IL in Fig. 8(b). As shown in Fig. 8(b), $\Delta\nu$(C=C) increased with an increase in the pK_a value of the ligand IL. The high vibration frequency of the aromatic C=C bond caused an increase in the electron density of the C=C bond [64,65]. Therefore, it was confirmed that the π electron density of the aromatic ring of Co(salen)-type MCILs increased with an increase in the pK_a value of the ligand ILs. Specifically, the high viscosity of Co(salen)-type MCILs having ligand ILs with high pK_a was caused by the high π electron density of the equatorial ligand due to strong σ electron donation from the ligand ILs. Unfortunately, for the Co(acacen)-type MCILs, the peak of C=C vibration, which should be observed near 1570 cm^{-1} [40], was overlapped by other peaks and could not be assigned (Fig. S8). However, the π electron density of the equatorial ligand of Co(acacen)-type MCILs might be increased with an increase in the pK_a value of the ligand ILs because the acacen ligand also withdraws electrons from the Co atom[47]. Therefore, the viscosity of Co(acacen)-type MCILs might increase with an increase in the pK_a of the ligand ILs.

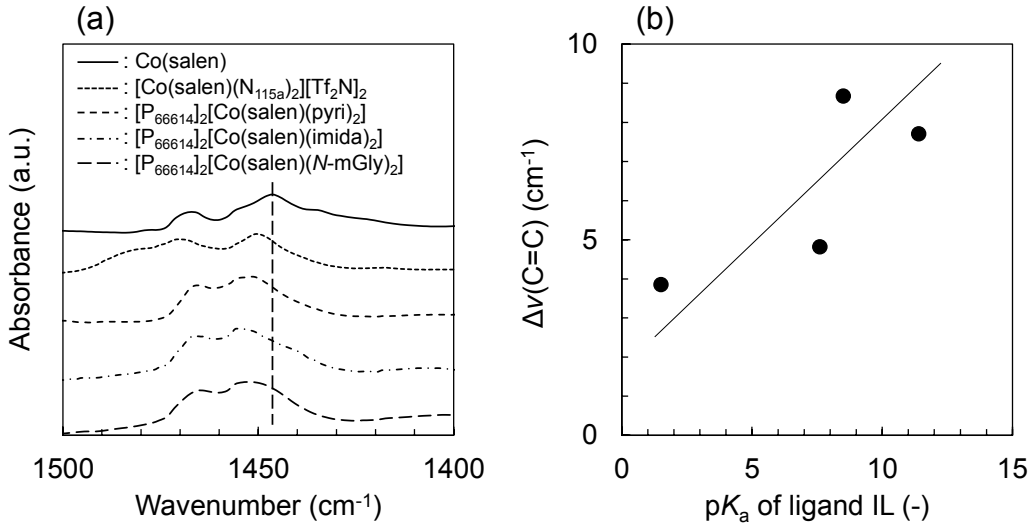

Fig. 8 (a) FT-IR spectra of each Co(salen)-type MCIL with different ligand ILs and neat Co(salen) complex around 1450 cm^{-1}. (b) Relationship between $\Delta\nu$(C=C) and pK_a of the ligand ILs measured by the acid-base titration test.

To confirm the effect of the pK_a value of ligand ILs on the viscosity of Co(acacen)-type MCILs, the relationship between the viscosity of Co(acacen)-type MCILs and the chemical structure of ligand ILs was systematically investigated using MCILs having the form $[N_{R1R1R2(na)}][Tf_2N]$, with different methylene groups as the ligand ILs. Here, "n" of $[N_{R1R1R2(na)}][Tf_2N]$ means the number of methylene groups, "a" denotes the amino group, and R_1 and R_2 denote alkyl chains (Fig. 2). The pK_a of $[N_{R1R1R2(na)}][Tf_2N]$ can be controlled by changing the number of methylene groups.

It should be noted that the number of methylene groups has another effect on the chemical structure of $[Co(acacen)(N_{R1R1R2(na)})_2][Tf_2N]_2$. An increase in the number of methylene groups results in an increase in the distance between the two cations of $[Co(acacen)(N_{R1R1R2(na)})_2][Tf_2N]_2$. Shirota et al. reported that the distance between the two cations of gemini-type ILs had little effect on the viscosity of gemini-type ILs[66]. Therefore, it can be considered that a change in the distance between the two cations of $[Co(acacen)(N_{R1R1R2(na)})_2][Tf_2N]_2$ hardly affects the viscosity of MCILs. In other words, the effect of the ligand IL pK_a on the viscosity of Co(acacen)-type MCILs could be investigated by using $[Co(acacen)(N_{R1R1R2(na)})_2][Tf_2N]_2$ with different methylene groups of the ligand ILs.

Fig. 9 shows the relationship between the pK_a value of ligand ILs and the viscosities of several $[Co(acacen)(N_{R1R1R2(na)})_2][Tf_2N]_2$. The p$K_a$ of the ligand ILs and the viscosity of the MCILs used in Fig. 9 are listed in Table S4 to associate each MCIL with its values. As expected, the viscosity of $[Co(acacen)(N_{111(na)})_2][Tf_2N]_2$, $[Co(acacen)(N_{115(na)})_2][Tf_2N]_2$, and $[Co(acacen)(N_{225(na)})_2][Tf_2N]_2$ increased with an increase in the pK_a value of the ligand ILs because of the increase in the electron density of the equatorial ligand of Co(acacen)-type MCILs.

In conclusion, the interaction among MCIL molecules due to the π electron system would be the dominant factor affecting the viscosity of both types of MCILs. It was demonstrated that the strength of the interaction could be tuned by the π electron system of the equatorial ligands and the electron donation ability of the ligand ILs. Therefore, to develop MCILs with low viscosity, it is effective to use equatorial ligands with a small π electron systems and ligand ILs with low pK_a values.

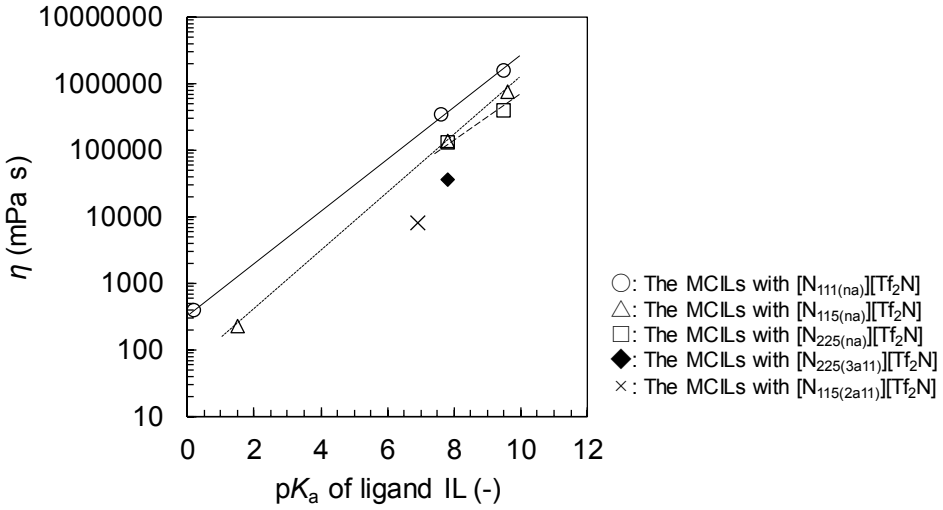

Fig. 9 Relationship between the viscosity of Co(acacen)-type MCILs and pK_a of the ligand ILs measured by the acid-base titration test in a methanol solution at 303.0 K.

3.3 Design criteria of MCILs with high O_2 absorbability and low viscosity

As O_2 absorbents, MCILs should have low N_2 absorbability, high O_2 reactivity, and low viscosity. For maximum N_2 absorption by MCILs, their molar volume is a critical factor. Because the molar volume of MCILs hardly affects their O_2 reactivity and viscosity (Figs. S11 and S12), N_2 absorbability can be independently controlled, regardless of the O_2 reactivity and viscosity of the MCILs. Therefore, it would be easy to design MCILs with low N_2 absorbability and either high O_2 reactivity or low viscosity.

In contrast, both O_2 reactivity and viscosity of the MCILs was affected by the pK_a of the ligand ILs. Because both O_2 absorbability and viscosity of the MCILs were increased with increasing ligand IL pK_a, as shown in Fig. 10, there was a trade-off relationship between the O_2 reactivity and viscosity of the MCILs. Thus, a MCIL with both high O_2 reactivity and low viscosity cannot be developed by only controlling the pK_a of the ligand ILs. In this section, we consider the design criteria for MCILs with both high O_2 reactivity and low viscosity.

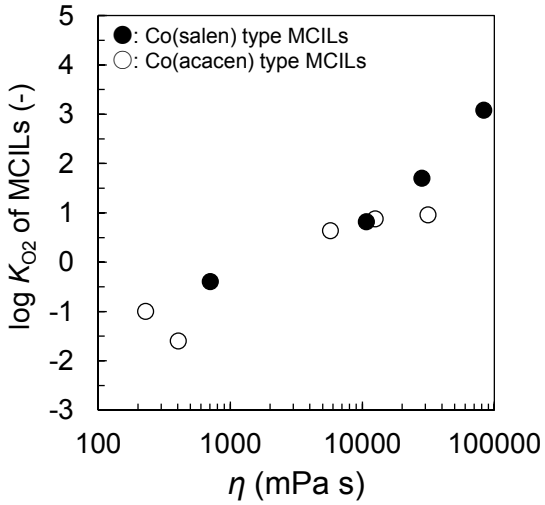

Fig. 10 Relationship between log K_{O2} and viscosity of both Co(salen) and Co(acacen)-type MCILs

O_2 reactivity of MCILs is determined by the electron density of the Co atom of MCILs. The electron density of the Co atom could be controlled by the pK_a of the ligand ILs. In contrast, MCIL viscosity was affected by the X-π interactions caused by the π electron system of the MCILs. The strength of the X-π interactions among the MCIL molecules might be controlled by the chemical structure of the π electron system and the X moiety, such as the introduction of the steric hindrance effect and the decrease in the number of interaction sites. It is expected that the chemical structure of the π electron system and X moiety could be designed without changing the pK_a of the ligand ILs. This means that the O_2 reactivity and viscosity of the MCILs might be controlled independently.

One possible alteration of the chemical structure of MCILs that weakens the X-π interactions is methylation of the amine group in the ligand ILs. Because the NH moiety in the MCILs disappeared by methylation of the amine group, the MCIL viscosity decreases because of the disappearance of the NH-π moiety. In fact, as shown in Fig. 9, comparing the viscosity of the MCILs with similar ligand IL pK_a values, the viscosity of [Co(acacen)($N_{115(2a11)}$)$_2$][Tf_2N]$_2$ and [Co(acacen)($N_{225(3a11)}$)$_2$][Tf_2N]$_2$ without the NH moiety were lower those that of the MCILs with the NH moiety. This result demonstrated that X-π interactions could be controlled by altering the chemical structure of the X moiety.

The criterion for designing MCILs with both high O_2 reactivity and low viscosity is the suppression of X-π interactions without decreasing the electron density of the Co atom. Fundamentally, the source of X-π interactions was the π electron system of the equatorial ligand of MCILs. Therefore, optimizing the chemical structure of the equatorial ligand, such as by decreasing the π electron system and introducing steric hindrance to the π electron system[67], is important for further improvement of the performance of MCILs as O_2 absorbents. Designing the equatorial ligand to decrease the viscosity of MCILs while maintaining the O_2 absorbability is our next challenge.

4. Conclusions

To propose the optimal design criteria of MCILs that can act as effective O_2 absorbents, the amount of absorbed N_2, O_2 absorbability, and viscosity of the MCILs composed of Co(acacen) or Co(salen) complexes and different ligand ILs were investigated. Based on the relationship between the chemical structure of the MCILs and each property, the dominant factors that determine each property of the MCILs were investigated.

The amount of N_2 absorbed in the MCILs was strongly affected by the molar volume of the MCILs. The use of small ligand ILs and metal complexes is effective to decrease the amount of absorbed N_2. In contrast, the O_2 absorbability of the MCILs showed good correlation with the pK_a of the ligand ILs, which indicated that the O_2 absorbability was strongly affected by the electron density of the Co atom of the MCILs. The electron density of the Co atom could be enhanced by using ligand ILs with strong electron donation ability. The X-π interactions (X: cation, NH, CH, and π system) due to the π electron system of the equatorial ligands played an important role in determining the MCIL viscosity. The decrease of this interaction brought about a decrease in viscosity.

Based on above-mentioned factors, it can be said that designing chemical structures of MCILs to weaken the X-π interactions is quite important to develop MCILs with low N_2 absorbability, high O_2 reactivity, and low viscosity. Decreasing the π electron system and introducing steric hindrance to the π electron system might be effective to obtain the desired chemical structure of the equatorial ligand.

5. Acknowledgment

Part of this work was supported by JSPS KAKENHI (Grant Number 19J11532) and the Adaptable and Seamless Technology Transfer Program through Target-driven R&D (A-STEP) (VP30118067714) from the Japan Science and Technology Agency (JST).

6. References

[1] P. Bernardo, E. Drioli, G. Golemme, Membrane gas separation: A review/state of the art, Ind. Eng. Chem. Res. 48 (2009) 4638–4663.

[2] F. Wu, M.D. Argyle, P.A. Dellenback, M. Fan, Progress in O_2 separation for oxy-fuel combustion–A promising way for cost-effective CO_2 capture: A review, Prog. Energy Combust. Sci. 67 (2018) 188–205.

[3] T. Burdyny, H. Struchtrup, Hybrid membrane/cryogenic separation of oxygen from air for use in the oxy-fuel process, Energy. 35 (2010) 1884–1897.

[4] H. Lin, M. Zhou, J. Ly, J. Vu, J.G. Wijmans, T.C. Merkel, J. Jin, A. Haldeman, E.H. Wagener, D. Rue, Membrane-based oxygen-enriched combustion, Ind. Eng. Chem. Res. 52 (2013) 10820–10834.

[5] J.-G. Jee, J.-S. Lee, C.-H. Lee, Air Separation by a Small-Scale Two-Bed Medical O_2 Pressure Swing Adsorption, Ind. Eng. Chem. Res. 40 (2001) 3647–3658.

[6] P.D. Southon, D.J. Price, P.K. Nielsen, C.J. McKenzie, C.J. Kepert, Reversible and selective O_2 chemisorption in a porous metal-organic host material, J. Am. Chem. Soc. 133 (2011) 10885–10891.

[7] J.R. Li, R.J. Kuppler, H.C. Zhou, Selective gas adsorption and separation in metal-organic frameworks, Chem. Soc. Rev. 38 (2009) 1477–1504.

[8] J.-R. Li, J. Sculley, H.-C. Zhou, Metal–Organic Frameworks for Separation, Chem. Rev. 112 (2012) 869–932.

[9] D.J. Xiao, M.I. Gonzalez, L.E. Darago, K.D. Vogiatzis, E. Haldoupis, L. Gagliardi, J.R. Long, Selective, Tunable O_2 Binding in Cobalt(II)-Triazolate/Pyrazolate Metal-Organic Frameworks, J. Am. Chem. Soc. 138 (2016) 7161–7170.

[10] D.F. Sava Gallis, M. V. Parkes, J.A. Greathouse, X. Zhang, T.M. Nenoff, Enhanced O_2 selectivity versus N_2 by partial metal substitution in Cu-BTC, Chem. Mater. 27 (2015) 2018–2025.

[11] L.J. Murray, M. Dinca, J. Yano, S. Chavan, F. Bonino, S. Bordiga, C.M. Brown, J.R. Long, Highly-Selective and Reversible O_2 Binding in Cr_3(1,3,5-benzenetricarboxylate)$_2$, J. Am. Chem. Soc. 132 (2010) 7856–7857.

[12] W. Zhang, D. Banerjee, J. Liu, H.T. Schaef, J. V. Crum, C.A. Fernandez, R.K. Kukkadapu, Z. Nie, S.K. Nune, R.K. Motkuri, K.W. Chapman, M.H. Engelhard, J.C. Hayes, K.L. Silvers, R. Krishna, B.P. McGrail, J. Liu, P.K. Thallapally, Redox-Active Metal-Organic Composites for Highly Selective Oxygen Separation Applications, Adv. Mater. 28 (2016) 3572–3577.

[13] E.D. Bloch, L.J. Murray, W.L. Queen, S. Chavan, S.N. Maximoff, J.P. Bigi, R. Krishna, V.K. Peterson, F. Grandjean, G.J. Long, B. Smit, S. Bordiga, C.M. Brown, J.R. Long, Selective binding of O_2 over N_2 in a redox-active metal-organic framework with open iron(II) coordination sites, J. Am. Chem. Soc. 133 (2011) 14814–14822.

[14] T. Zhao, X. Zhang, Z. Tu, Y. Wu, X. Hu, Low-viscous diamino protic ionic liquids with fluorine-substituted phenolic anions for improving CO_2 reversible capture, J. Mol. Liq. 268 (2018) 617–624.

[15] J.F. Huang, H. Luo, C. Liang, D.E. Jiang, S. Dai, Advanced liquid membranes based on novel ionic liquids for selective separation of olefin/paraffin via olefin-facilitated transport, Ind. Eng. Chem. Res. 47 (2008) 881–888.

[16] S. Seo, M. Quiroz-Guzman, M.A. Desilva, T.B. Lee, Y. Huang, B.F. Goodrich, W.F. Schneider, J.F. Brennecke, Chemically tunable ionic liquids with aprotic heterocyclic anion (AHA) for CO_2 capture, J. Phys. Chem. B. 118 (2014) 5740–5751.

[17] S. Zeng, X. Zhang, L. Bai, X. Zhang, H. Wang, J. Wang, D. Bao, M. Li, X. Liu, S. Zhang, Ionic-Liquid-Based CO_2 Capture Systems: Structure, Interaction and Process, Chem. Rev. 117 (2017) 9625–9673.

[18] X. Zhang, X. Zhang, H. Dong, Z. Zhao, S. Zhang, Y. Huang, Carbon capture with ionic liquids: overview and progress, Energy Environ. Sci. 5 (2012) 6668–6681.

[19] L.Y. Wang, Y.L. Xu, Z.D. Li, Y.N. Wei, J.P. Wei, CO_2/CH_4 and H_2S/CO_2 Selectivity by Ionic Liquids in Natural Gas Sweetening, Energy and Fuels. 32 (2018) 10–23.

[20] F. Karadas, M. Atilhan, S. Aparicio, Review on the use of ionic liquids (ILs) as alternative fluids for CO_2 capture and natural gas sweetening, Energy and Fuels. 24 (2010) 5817–5828.

[21] T. Torimoto, T. Tsuda, K.I. Okazaki, S. Kuwabata, New frontiers in materials science opened by ionic liquids, Adv. Mater. 22 (2010) 1196–1221.

[22] R.D. Rogers, K.R. Seddon, Ionic Liquids-Solvents of the Future?, Science. 302 (2003) 792–793.

[23] R.L. Vekariya, A review of ionic liquids: Applications towards catalytic organic transformations, J. Mol. Liq. 227 (2017) 44–60.

[24] S. Kasahara, E. Kamio, H. Matsuyama, Improvements in the CO_2 permeation selectivities of amino acid ionic liquid-based facilitated transport membranes by controlling their gas absorption properties, J. Memb. Sci. 454 (2014) 155–162.

[25] Z. Fei, T.J. Geldbach, D. Zhao, P.J. Dyson, From dysfunction to bis-function: On the design and applications of functionalised ionic liquids, Chem. A Eur. J. 12 (2006) 2122–2130.

[26] E.D. Bates, R.D. Mayton, I. Ntai, J.H. Davis, CO_2 capture by a task-specific ionic liquid, J. Am. Chem. Soc. 124 (2002) 926–927.

[27] D.E. Jiang, S. Dai, First principles molecular dynamics simulation of a task-specific ionic liquid based on silver-olefin complex: Atomistic insights into a separation process, J. Phys. Chem. B. 112 (2008) 10202–10206.

[28] P. Nockemann, B. Thijs, T.N. Parac-Vogt, K. Van Hecke, L. Van Meervelt, B. Tinant, I. Hartenbach, T. Schleid, V.T. Ngan, M.T. Nguyen, K. Binnemans, Carboxyl-Functionalized Task-Specific Ionic Liquids for Solubilizing Metal Oxides, Inorg. Chem. 47 (2008) 9987–9999.

[29] I. Newington, J.M. Perez-Arlandis, T. Welton, Ionic liquids as designer solvents for nucleophilic aromatic substitutions, Org. Lett. 9 (2007) 5247–5250.

[30] F. Moghadam, E. Kamio, H. Matsuyama, High CO_2 separation performance of amino acid ionic liquid-based double network ion gel membranes in low CO_2 concentration gas mixtures under humid conditions, J. Memb. Sci. 525 (2017) 290–297.

[31] S. Kasahara, E. Kamio, T. Ishigami, H. Matsuyama, Amino acid ionic liquid-based facilitated transport membranes for CO_2 separation, Chem. Commun. 48 (2012) 6903–6905.

[32] H. Fu, X. Wang, H. Sang, R. Fan, Y. Han, J. Zhang, Z. Liu, The study of bicyclic amidine-based ionic liquids as promising carbon dioxide capture agents, J. Mol. Liq. 304 (2020) 112805.

[33] P. Mehta, S. Vedachalam, G. Sathyaraj, S. Garai, G. Arthanareeswaran, K. Sankaranarayanan, Fast sensing ammonia at room temperature with proline ionic liquid incorporated cellulose acetate membranes, J. Mol. Liq. 305 (2020) 112820.

[34] T. Zhao, P. Li, X. Feng, X. Hu, Y. Wu, Study on absorption and spectral properties of H_2S in carboxylate protic ionic liquids with low viscosity, J. Mol. Liq. 266 (2018) 806–813.

[35] A. Matsuoka, E. Kamio, T. Mochida, H. Matsuyama, Facilitated O_2 transport membrane containing Co(II)-salen complex-based ionic liquid as O_2 carrier, J. Memb. Sci. 541 (2017) 393–402.

[36] A. Matsuoka, E. Kamio, H. Matsuyama, Investigation into the Effective Chemical Structure of Metal-Containing Ionic Liquids for Oxygen Absorption, Ind. Eng. Chem. Res. 58 (2019) 23304–23316.

[37] Q. Zheng, S.J. Thompson, S. Zhou, M. Lail, K. Amato, A. V. Rayer, J. Mecham, P. Mobley, J. Shen, B. Fletcher, Task-Specific Ionic Liquids Functionalized by Cobalt(II) Salen for Room Temperature Biomimetic Dioxygen Binding, Ind. Eng. Chem. Res. 58 (2019) 334–341.

[38] K. Tsunashima, M. Sugiya, Physical and electrochemical properties of low-viscosity phosphonium ionic liquids as potential electrolytes, Electrochem. Commun. 9 (2007) 2353–2358.

[39] H.T. Clarke, B. Gillespie, S.Z. Weisshaus, The Action of Formaldehyde on Amines and Amino Acids, J. Am. Chem. Soc. 55 (1933) 4571–4587.

[40] K.C. Gupta, H.K. Abdulkadir, S. Chand, Polymer-immobilized N,N′-bis(acetylacetone)ethylenediamine cobalt(II) Schiff base complex and its catalytic activity in comparison with that of its homogenized analogue, J. Appl. Polym. Sci. 90 (2003) 1398–1411.

[41] M. Okuhata, T. Mochida, Ionic Liquids from the Cationic Cobalt(III) Schiff Base Complex, $[Co(acacen)L_2][Tf_2N]$ (acacen = N,N' bis(acetylacetone)ethylenediamine, Tf_2N = bis(trifluoromethanesulfonyl)amide), J. Coord. Chem. 67 (2014) 1361–1366.

[42] I. Canals, J.A. Portal, E. Bosch, M. Rosés, Retention of ionizable compounds on HPLC. 4. Mobile-phase pH measurement in methanol/water, Anal. Chem. 72 (2000) 1802–1809.

[43] Z. Lei, C. Dai, B. Chen, Gas solubility in ionic liquids, Chem. Rev. 114 (2014) 1289–1326.

[44] B. Dębski, A. Hänel, R. Aranowski, S. Stolte, M. Markiewicz, T. Veltzke, I. Cichowska-Kopczyńska, Thermodynamic interpretation and prediction of CO_2 solubility in imidazolium ionic liquids based on regular solution theory, J. Mol. Liq. 291 (2019).

[45] M.S. Shannon, J.M. Tedstone, S.P.O. Danielsen, M.S. Hindman, A.C. Irvin, J.E. Bara, Free volume as the basis of gas solubility and selectivity in imidazolium-based ionic liquids, Ind. Eng. Chem. Res. 51 (2012) 5565–5576.

[46] S. Seo, M.A. Desilva, H. Xia, J.F. Brennecke, Effect of Cation on Physical Properties and CO_2 Solubility for Phosphonium-Based Ionic Liquids with 2-Cyanopyrrolide Anions, J. Phys. Chem. B. 119 (2015) 11807–11814.

[47] M.J. Carter, D.P. Rillema, F. Basolo, Oxygen Carrier and Redox Properties of Some Neutral Cobalt Chelates. Axial and in-Plane Ligand Effects, J. Am. Chem. Soc. 96 (1974) 392–400.

[48] A. Pui, I. Berdan, I. Morgenstern-Badarau, A. Gref, M. Perrée-Fauvet, Electrochemical and spectroscopic characterization of new cobalt(II) complexes. Catalytic activity in oxidation reactions by molecular oxygen, Inorganica Chim. Acta. 320 (2001) 167–171.

[49] A.L. Crumbliss, F. Basolo, Monomeric Oxygen Adducts of N,N'-Ethylenebis(acetylacetoniminato)ligandcobalt (II), J. Am. Chem. Soc. 92 (1970) 55–60.

[50] G. Amiconi, G., Brunori, M., Antonini, E., Tauzher, G., Costa, Thermodynamics of the Reversible Oxygenation of Bis(Acetylacetone)-Ethylenediiminecobalt (II) in Pyridine, Nature. 228 (1970) 549–551.

[51] S. Patel, P. Patel, S.B. Undre, S.R. Pandya, M. Singh, S. Bakshi, DNA binding and dispersion activities of titanium dioxide nanoparticles with UV/vis spectrophotometry, fluorescence spectroscopy and physicochemical analysis at physiological temperature, J. Mol. Liq. 213 (2016) 304–311.

[52] D. Kumar, A. Chandra, M. Singh, Effect of $Pr(NO_3)_3$, $Sm(NO_3)_3$, and $Gd(NO_3)_3$ on Aqueous Solution Properties of Urea: A Volumetric, Viscometric, Surface Tension, and Friccohesity Study at 298.15 K and 0.1 MPa, J. Solution Chem. 45 (2016) 750–771.

[53] R. Chetty, M. Singh, In-vitro interaction of cerium oxide nanoparticles with hemoglobin, insulin, and dsDNA at 310.15 K: Physicochemical, spectroscopic and in-silico study, Int. J. Biol. Macromol. 156 (2020) 1022–1044.

[54] C. Janiak, A critical account on n-n stacking in metal complexes with aromatic nitrogen-containing ligands, J. Chem. Soc. Dalt. Trans. (2000) 3885–3896.

[55] M.K. Milčić, Z.D. Tomić, S.D. Zarić, Very strong metal ligand aromatic cation-π interactions in transition metal complexes: Intermolecular interaction in tetraphenylborate salts, Inorganica Chim. Acta. 357 (2004) 4327–4329.

[56] H. Keypour, M. Shayesteh, M. Rezaeivala, F. Chalabian, Y. Elerman, O. Buyukgungor, Synthesis, spectral characterization, structural investigation and antimicrobial studies of mononuclear Cu(II), Ni(II), Co(II), Zn(II) and Cd(II) complexes of a new potentially hexadentate N_2O_4 Schiff base ligand derived from salicylaldehyde, J. Mol. Struct. 1032 (2013) 62–68.

[57] M.A.A.F. de, B. de Castro, A.M. Coelho, D. Domingues, C. Freire, J. Morais, Electrochemical and structural studies of nickel(II) complexes with N_2O_2 Schiff base ligands derived from 2-hydroxy-1-naphthaldehyde. Molecular structure of N,N′-2,3-dimethylbutane-2,3-diyl-bis(2-hydroxy-1-naphthylideneiminate) nickel(II), Inorganica Chim. Acta. 205 (1993) 157–166.

[58] A. Gutiérrez, M.F. Perpiñán, A.E. Sánchez, M.C. Torralba, M.R. Torres, Stabilization of the cobalt coordination site in transmetalation processes on dinuclear salen derivatives, Inorganica Chim. Acta. 363 (2010) 1837–1842.

[59] C.A. Hunter, J.K.M. Sanders, The Nature of π-π Interactions, J. Am. Chem. Soc. 112 (1990) 5525–5534.
[60] N. Mahata, A.R. Silva, M.F.R. Pereira, C. Freire, B. de Castro, J.L. Figueiredo, Anchoring of a [Mn(salen)Cl] complex onto mesoporous carbon xerogels, J. Colloid Interface Sci. 311 (2007) 152–158.
[61] X. Mei, C. Wolf, Highly congested nondistorted diheteroarylnaphthalenes: Model compounds for the investigation of intramolecular π-stacking interactions, J. Org. Chem. 70 (2005) 2299–2305.
[62] M.A. Muñoz, O. Sama, M. Galán, P. Guardado, C. Carmona, M. Balón, Hydrogen bonding NH/π interactions between betacarboline and methyl benzene derivatives, Spectrochim. Acta - Part A Mol. Biomol. Spectrosc. 57 (2001) 1049–1056.
[63] A.H. Kianfar, L. Keramat, M. Dostani, M. Shamsipur, M. Roushani, F. Nikpour, Synthesis, spectroscopy, electrochemistry and thermal study of Ni(II) and Cu(II) unsymmetrical N_2O_2 Schiff base complexes, Spectrochim. Acta - Part A Mol. Biomol. Spectrosc. 77 (2010) 424–429.
[64] E.M. Nour, A.A. Taha, I.S. Alnaimi, Infrared and Raman studies of [UO_2(salen)(L)] (L=H_2O and CH_3OH), Inorganica Chim. Acta. 141 (1988) 139–144.
[65] M. Tsuboi, Y. Kyogoku, T. Shimanouchi, Infrared absorption spectra of protonated and deprotonated nucleosides, Biochim. Biophys. Acta. 55 (1962) 1–12.
[66] H. Shirota, T. Mandai, H. Fukazawa, T. Kato, Comparison between dicationic and monocationic ionic liquids: Liquid density, thermal properties, surface tension, and shear viscosity, J. Chem. Eng. Data. 56 (2011) 2453–2459.
[67] S. Biradar, R. Kasugai, H. Kanoh, H. Nagao, Y. Kubota, K. Funabiki, M. Shiro, M. Matsui, Liquid azo dyes, Dye. Pigment. 125 (2016) 249–258.